International Journal of Tomography & Statistics (IJTS),
Fall 2006, Vol. 4, No. F06; Int. J. Tomogr. Stat.; 5-16
ISSN 0972-9976;

A comparison of the imaging conditions and principles in depth migration algorithms

Bogdan G. Nita

Department of Mathematical Sciences
Montclair State University
1 Normal Avenue, Montclair, New Jersey, 07043, USA
nitab@mail.montclair.edu

ABSTRACT

Seismic migration/inversion is presently the most used method for determining the structure and properties of the sub-surface in seismic exploration for hydrocarbons. Determining the location of abrupt changes in medium's parameters involves, in one form or another, an imaging principle which can simply be stated by equating a component, or the full value of the travel-time t, with zero. Depending on the domain of definition of the imaged data, i.e. space-frequency or wavenumber-frequency, the imaging step has different implications, capabilities and produces different results. We analyze this principle for the depth migration procedures and point out that the space-frequency algorithms imply a total travel-time condition $t = 0$ while the wavenumber-frequency algorithms imply vertical intercept time condition $\tau = 0$. We present two analytic examples of the most common migration algorithms for both domains, i.e. $f - k$ migration for the wavenumber-frequency and Kirchhoff for the space-frequency algorithms. In addition, we discuss the implications of the different imaging principle that these algorithms use.

Keywords: Imaging conditions, seismic depth migration, space frequency and wavenumber frequency migration.

2000 Mathematics Subject Classification: 86A22, 35J05.

1 Introduction

Seismic migration represents the shifting and focusing of the recorded reflections to their true position thus creating an image of the sub-surface under investigation. Most of the depth migration algorithms can be viewed as a two-step procedure in which the geophysical data is first downward-extrapolated to any depth and then imaged to its correct location by using an imaging principle. Depending on the domain in which the second step (imaging) is performed the algorithms can be divided into two broad categories: 1. space-frequency algorithms e.g. Kirchhoff (Schneider, 1978), 15° finite differences (Claerbout, 1981) etc. and 2. wavenumber-frequency algorithms e.g. phase-shift migration (Gazdag, 1978), $f - k$ migration (Stolt, 1978) etc. In this paper we compare the imaging step involved in these two types of algorithms and point out that the imaging condition in the space-frequency domain amounts to imposing a zero total travel time condition $t = 0$, while the imaging condition in the wavenumber-frequency

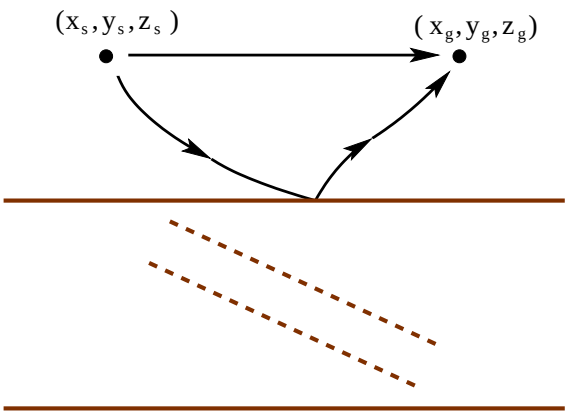

Figure 1: A typical seismic experiment over a multi-dimensional, i.e. (x, y, z)-varying, earth. The dashed lines in the pictures indicate any degree of simple and complex variations in earth parameters, e.g. wave speed, density, etc.

domain amounts to imposing zero vertical intercept time condition $\tau = 0$. The two categories of migration algorithms have been illustrated through numerical results extensively in the literature, see e.g. (Yilmaz, 2001). Rather than providing redundant numerical instances, we find it useful to present two analytic examples which show some of the similarities and differences between the two types of algorithms. Given the wide application of the migration algorithms, it is important to have a good grasp and understanding of the mathematics and physics associated with their formulation. This in turn leads to a better understanding of their capability and consequently to the development of more accurate and complete imaging methods. This research impacts not only the migration methods but also other algorithms which implicitly use an imaging principle in their formulation, e.g. inverse scattering methods and in particular internal multiple attenuation and imaging algorithms (Weglein, Araújo, Carvalho, Stolt, Matson, Coats, Corrigan, Foster, Shaw and Zhang, 2003). We begin by describing the relationship between spherical waves and their Fourier planewave decomposition and concentrate on understanding the geometry and elements of one planewave component. We then briefly review two of the most common migration algorithms representative for the wavenumber-frequency and space-frequency domains, namely $f - k$ migration and Kirchhoff migration. We finally provide analytic examples for acoustic 1.5-D models emphasizing the imaging step in each of the two procedures. Conclusions are drawn in the last section.

2 Spherical waves and Fourier planewave decomposition

A typical seismic experiment involves man-made sources, of acoustic or elastic disturbances, and receivers, to capture these disturbances after traveling through the earth and interacting with different internal structures (see Figure 1). For a 3-dimensional acoustic inhomogeneous

medium, with sources and receivers located on the earth surface at $z_s = z_g = 0$, and with the horizontal coordinates $\mathbf{x_s} = (x_s, y_s)$ and $\mathbf{x_g} = (x_g, y_g)$ respectively, the propagation of the waves through the medium is described by the Helmoltz equation

$$\nabla^2 P - \frac{1}{c^2}\frac{\partial^2 P}{\partial t^2} = -4\pi\delta(\mathbf{x_g} - \mathbf{x_s})\delta(t) \tag{2.1}$$

where P represents an acoustic wave propagating through an inhomogeneous medium whose spatially varying velocity is given by the function c and δ is the Dirac delta function. The homogeneous space ($c = c_0$) solution or the direct arrival can be described by

$$P_h(\mathbf{x_g}, z_g = 0, \mathbf{x_s}, z_s = 0, \omega) = \frac{e^{i\omega\frac{R}{c_0}}}{R} \tag{2.2}$$

where we have assumed the source and receiver to be located at depths $z_s = z_g = 0$ and where $R = \|\mathbf{x_g} - \mathbf{x_s}\| = \sqrt{(x_g - x_s)^2 + (y_g - y_s)^2}$ represents the distance between the source and receiver. Solutions corresponding to other arrivals can be obtained by adding boundary conditions describing the internal structure of the medium under investigation. For each abrupt change in the medium parameter, or interface, the incoming wave is broken down into a reflected and a transmitted wave, which satisfy the continuity conditions with regards to pressure and displacement. The recorded data

$$D(\mathbf{x_g}, \mathbf{x_s}, \omega) = P(\mathbf{x_g}, 0, \mathbf{x_s}, 0, \omega) \tag{2.3}$$

consists in all possible seismic arrivals which result from such internal interactions.
Equation (2.1) can also be solved using Fourier transform methods (Aki and Richards, 2002) to obtain the solutions in the Weyl integral form. The homogeneous solution will then have the form

$$P_h(\mathbf{x_g}, 0, \mathbf{x_s}, 0, \omega) = \frac{1}{2\pi i}\int_{-\infty}^{\infty} d\mathbf{k_g}\int_{-\infty}^{\infty} d\mathbf{k_s}\frac{e^{i(\mathbf{k_g}\cdot\mathbf{x_g} - \mathbf{k_s}\cdot\mathbf{x_s})}}{k_z} \tag{2.4}$$

where $\mathbf{k_s} = (k_{xs}, k_{ys})$ and $\mathbf{k_g} = (k_{xg}, k_{yg})$ are the source and receiver horizontal wavenumbers and where we used different sign convention for the Fourier transform over the source and receiver coordinates. Here $k_z = q_s + q_g$ with q_s and q_g being the vertical source and receiver wavenumbers respectively, satisfying the dispersion relationships

$$q_g^2 + \|\mathbf{k_g}\|^2 = q_s^2 + \|\mathbf{k_s}\|^2 = \omega^2/c_0^2. \tag{2.5}$$

This solution can be interpreted as a continuous summation over all planewaves described by the horizontal wavenumbers $\mathbf{k_g}$ and $\mathbf{k_s}$. Each individual planewave satisfies the Fourier transformed Helmoltz equation and, in the presence of boundary condition, can be interpreted as the medium response to incoming planewaves. The data in this case will be the set of collected planewave events on the measurement surface and will be expressed through

$$\tilde{D}(\mathbf{k_g}, \mathbf{k_s}, \omega). \tag{2.6}$$

It is not difficult to see that the relationship between D and $\tilde{D}$ is

$$D(\mathbf{x_g}, \mathbf{x_s}, t) = \int_{-\infty}^{\infty} d\omega\int_{-\infty}^{\infty} d\mathbf{k_g}\int_{-\infty}^{\infty} d\mathbf{k_s} e^{-i(\omega t - \mathbf{k_g}\cdot\mathbf{x_g} + \mathbf{k_s}\cdot\mathbf{x_s})}\tilde{D}(\mathbf{k_g}, \mathbf{k_s}, \omega). \tag{2.7}$$

Notice that, to construct the point-source/point-receiver response, all the horizontal wavenumbers dependent planewave components are needed. The same is not true, for example, for a ray approximation where each event in the point-source/point-receiver response is approximated by one ray-like diagram. In the next section we discuss one planewave component and look at its geometry, propagation and ways of characterizing its turning point or reflection from an interface.

3 The geometry of planewaves

Figure 2 shows a planewave component with the typical quantities attached to it, i.e. the angle of incidence θ, the ray perpendicular to the wavefront indicating the direction of propagation, the velocity of propagation of the planewave c_0 and the vertical and horizontal intercept velocities c_v and c_h. The intercept velocities are dependent on the incidence angle θ and usually are larger than c_0 (with the exception of vertical or horizontal propagation in which case one of them is equal to c_0 and the other is zero) and for oblique incidence have the expressions

$$c_h = \frac{c_0}{\sin\theta} \tag{3.1}$$

and

$$c_v = \frac{c_0}{\cos\theta}. \tag{3.2}$$

The quantities $\frac{1}{c_h}$ and $\frac{1}{c_v}$ are called the horizontal and vertical slowness respectively and are denoted by p and q. The wavefront of the planewave can be viewed as an infinite line in the $z-x$ domain having the equation

$$z = z_0 - x\tan\theta \tag{3.3}$$

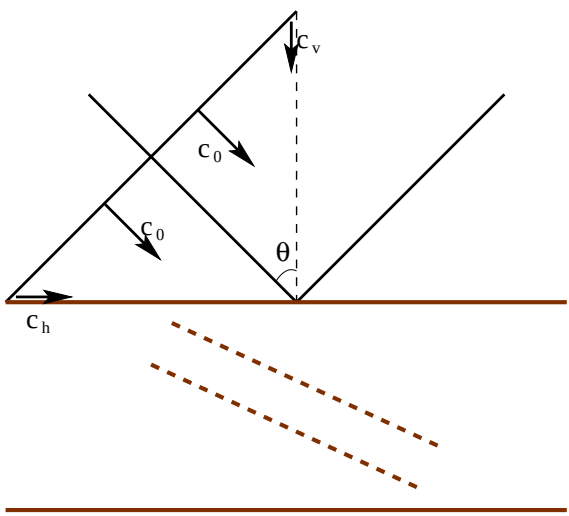

Figure 2: A plane wave component: downgoing ray and wavefront.

where z_0 is the intercept between the front of the planewave and the vertical axis. To indicate that the planewave is moving downward it is necessary to have only this z-intercept advance on the vertical axis as

$$z = c_v t - x \tan\theta, \tag{3.4}$$

where t is the traveltime, or

$$z = c_0 \frac{t}{\cos\theta} - x \tan\theta. \tag{3.5}$$

Solving for the total travel-time from equation (3.5) we find

$$t = z\frac{\cos\theta}{c_0} + x\frac{\sin\theta}{c_0}. \tag{3.6}$$

The quantity

$$\tau_s = z\frac{\cos\theta}{c_0} \tag{3.7}$$

is called the vertical intercept time and has the units of time (seconds). The subscript s indicates the fact that the quantity is specific to the source-reflector leg. A similar expression, possibly with a different reflection angle, can be written for τ_g, the vertical time for the reflector-receiver leg. The total vertical time for the planewave seismic event is defined as

$$\tau = \tau_s + \tau_g. \tag{3.8}$$

In terms of the vertical time τ_s and the horizontal slowness p defined above, equation (3.6) can now be re-written as

$$t = \tau_s + xp. \tag{3.9}$$

Equation (3.6) describes the time at which the planewave will pass any (x, z) point in the 2-dimensional plane. To describe the time shift of this planewave as it moves along its ray from the source to the receiver, we represent the planewave as

$$\phi = e^{-i\omega(t-t_0)} = e^{-i\omega(t - z\frac{\cos\theta}{c_0} - x\frac{\sin\theta}{c_0})}. \tag{3.10}$$

A similar expression can be written for the reflector-to-receiver leg of the planewave propagation. Comparing this relation with the kernel of the Fourier transform in the expression (2.7) we discover the relations between the horizontal wavenumbers and the incidence angle

$$\sin\theta = \frac{\|\mathbf{k_s}\|}{\omega/c_0} \tag{3.11}$$

and

$$\cos\theta = \frac{q_s}{\omega/c_0}. \tag{3.12}$$

Eliminating the angle between equations (3.12) and (3.7) we find

$$\tau_s = z\frac{q_s}{\omega}. \tag{3.13}$$

Similarly for the reflection-receiver leg we can write

$$\tau_g = z\frac{q_g}{\omega} \tag{3.14}$$

or, after adding the two equations

$$\tau = \frac{k_z z}{\omega}. \tag{3.15}$$

As expected, the vertical intercept time of a planewave is only dependent on the vertical wavenumber k_z, the depth coordinate z and the frequency ω.
The importance of equation (3.15) comes from the fact that the expression $k_z z$ is the phase used to downward extrapolate planewave components in wavenumber-frequency seismic depth migration. Such a relation shows that the time component which varies in the downward extrapolation step is the vertical intercept time and it also offers a hint for interpreting the integration over frequency in the imaging principle. This concept along with the imaging conditions in wavenumber-frequency and space-frequency domains will be discussed in the following sections.

4 Pre-stack depth migration algorithms

We start with the data set $D(\mathbf{x_g}|\mathbf{x_s};t)$ depending on the source and receiver horizontal coordinates $\mathbf{x_s} = (x_s, y_s)$ and $\mathbf{x_g} = (x_g, y_g)$ and the total travel-time t measured from the source's explosion. For simplicity we assume that both sources and receivers are located on the earth's surface at depth $z = 0$. The data can then be represented as a wavefield P such that

$$P(\mathbf{x_g}, 0|\mathbf{x_s}, 0; t) = D(\mathbf{x_g}|\mathbf{x_s}; t). \tag{4.1}$$

To downward extrapolate this wave field we first Fourier transform it to the wavenumber-frequency domain

$$P(\mathbf{k_g}, 0|\mathbf{k_s}, 0; \omega) = \int d\mathbf{x_g} d\mathbf{x_s} dt e^{i(\omega t - \mathbf{k_g}\cdot\mathbf{x_g} + \mathbf{k_s}\cdot\mathbf{x_s})} P(\mathbf{x_g}, 0|\mathbf{x_s}, 0; t), \tag{4.2}$$

where we used different sign conventions for Fourier transforms over source and receiver coordinates. In the formula above $\mathbf{k_g} = (k_{xg}, k_{yg})$ and $\mathbf{k_s} = (k_{xs}, k_{ys})$ are the horizontal wavenumbers associated with the source and receiver horizontal positions $\mathbf{x_s}$ and $\mathbf{x_g}$ respectively. The effect of these transformations is a mono-chromatic planewave decomposition of the recoded signal. The quantity $P(\mathbf{k_g}, 0|\mathbf{k_s}, 0; \omega)$ can be viewed as the medium's response, recorded on the measurement surface, due to a set of planewaves characterized by the frequency ω and the horizontal wavenumbers $\mathbf{k_s}$ (from the source surface to the reflector) and $\mathbf{k_g}$ (from the reflector to the measurement surface). The wavefront of any such planewave is an infinite plane in the xyz space whose upward or downward propagation is described by the advance of the $z-$intercept on the vertical axis. In other words, in the wavenumber-frequency domain, the phase of any event will account only for this up-down propagation. As a consequence, the planewave response can be downward extrapolated by using a phase-shift operator on the vertical component only

$$P(\mathbf{k_g}, z|\mathbf{k_s}, z; \omega) = P(\mathbf{k_g}, 0|\mathbf{k_s}, 0; \omega) e^{ik_z z} \tag{4.3}$$

where, as before, $k_z = q_s + q_g$ and q_s and q_g are the medium dependent vertical source and receiver wavenumbers respectively. As emphasized earlier, since the only space component

that varies in the downward extrapolation process is the z-intercept, it is clear that the only variable time component is the vertical intercept time τ (see equation (3.15))

$$\tau = k_z z/\omega. \tag{4.4}$$

Summing over all frequency components, by performing either an integral over ω, (Gazdag, 1978), or over k_z, (Stolt, 1978), while the data is in the wavenumber-frequency domain is thus equivalent to a vertical intercept time $\tau = 0$ imaging condition. The last step in the migration procedure is an inverse Fourier transform over the horizontal wavenumbers to convert the imaged data back to the space domain. The result of this transformation is an image, denoted I_1, of the subsurface

$$I_1(x, y, z) = \int d\mathbf{k_g} d\mathbf{k_s} e^{i(\mathbf{k_g}-\mathbf{k_s})\cdot\mathbf{x}} d\omega P(\mathbf{k_g}, z|\mathbf{k_s}, z; \omega). \tag{4.5}$$

where $\mathbf{x}$ denotes the horizontal position vector (x, y). The full migration procedure can hence be written as

$$I_1(x, y, z) = \int d\mathbf{k_g} d\mathbf{k_s} e^{i(\mathbf{k_g}-\mathbf{k_s})\cdot\mathbf{x}} d\omega e^{ik_z z} \int d\mathbf{x_g} d\mathbf{x_s} dt e^{i(\omega t - \mathbf{k_g}\cdot\mathbf{x_g} + \mathbf{k_s}\cdot\mathbf{x_s})} D(\mathbf{x_g}|\mathbf{x_s}; t). \tag{4.6}$$

To obtain a version of this migration procedure in the space-frequency domain we re-arrange the order of integration in formula (4.6) while keeping the data in the frequency domain to obtain

$$I_2(x, y, z) = \int d\mathbf{x_g} d\mathbf{x_s} d\omega D(\mathbf{x_g}|\mathbf{x_s}; \omega) \int d\mathbf{k_g} d\mathbf{k_s} e^{i(k_z z - \mathbf{k_g}\cdot(\mathbf{x_g}-\mathbf{x}) + \mathbf{k_s}\cdot(\mathbf{x_s}-\mathbf{x}))}. \tag{4.7}$$

The last set of integrals over the horizontal wavenumbers is usually evaluated using a stationary phase approximation (Bleistein and Hendelsman, 1975) to obtain an approximative migration formula commonly called Kirchhoff migration, see e.g. (Schneider, 1978) and (Stolt and Benson, 1986). Formula (4.7) describes a weighted summation along diffraction hyperbolas in the original data. Since the data is now in the space-frequency domain, the phase of each event must account for both vertical and lateral propagation. This implies that an integration over frequency is equivalent to a total travel-time, $t = 0$, imaging condition.

The re-arrangement of integrals and their calculation in a different order have a significant effect, producing a different result in the two migration versions, and consequently a different image. This can be easily seen from the dispersion relations (2.5). For the wavenumber-frequency migration described by formula (4.6), the integral over ω is performed while keeping the horizontal wavenumbers constant. In this case, we can think of $(\mathbf{k_g}, \mathbf{k_s}, \omega)$ or $(\mathbf{k_g}, \mathbf{k_s}, k_z)$ as independent variables. It also implies that the vertical wavenumber k_z varies as a function of ω when performing the imaging step while $\mathbf{k_g}$ and $\mathbf{k_s}$ remain constant. For the space-frequency migration described by formula (4.7) the inner most integrals in $\mathbf{k_g}$ and $\mathbf{k_s}$ are performed while keeping the frequency constant. This implies that $\mathbf{k_g}$, $\mathbf{k_s}$ and k_z are no longer independent and one has to consider k_z as a function of both $\mathbf{k_g}$ and $\mathbf{k_s}$. Approximating the inner most integral in equation (4.7) using high frequency approximations (as one usually does in Kirchoff migration) results in a ray-path assumption for the seismic events and imposes a well defined relationship between the wavenumbers and frequency. This relation is used when integrating over frequencies and hence performing the imaging step in the space-frequency migration. These concepts will be made clearer in the analytic examples discussed below.

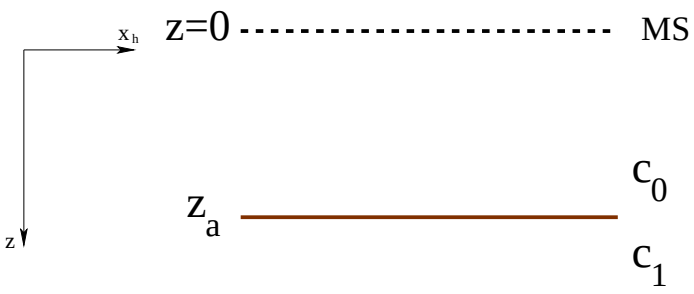

Figure 3: The model for the analytic 1.5D example. Sources and receivers in this experiment are located along the measurement surface (MS) which defines the horizontal $z = 0$ plane.

Imaging with the vertical intercept time $\tau = 0$ and with total travel-time $t = 0$ and the relation with the inverse scattering internal multiple attenuation algorithm was discussed by (Nita and Weglein, 2004) and (Nita and Weglein, 2005). They show that 1. the constant velocity pre-stack migration built into the algorithm is using a $\tau = 0$ imaging condition and 2. the pseudo-depth monotonicity condition can be translated into vertical time monotonicity. Both conclusions, along with the present research, are significant in understanding the efficiency, capabilities and limitations of the multiple attenuation algorithm and its different castings in other domains. The two analytic examples described below will further point out the advantages of using the $\tau = 0$ condition, or more generally, a wavenumber-frequency depth migration procedure.

5 Analytic example: wavenumber-frequency domain migration

Consider a one-dimensional model consisting of two half-spaces with the interface located at depth z_a (see Figure 3). The space-frequency domain data, $D(x_h; \omega)$, or the associated wavefield, $P(x_h, 0; \omega)$, for such an experiment can be expressed as

$$P(x_h, 0; \omega) = \frac{1}{2\pi} \int_{-\infty}^{\infty} dk_h \frac{R(k_h)}{ik_z} e^{ik_h x_h} e^{-ik_z z_a}, \tag{5.1}$$

see e.g. (Aki and Richards, 2002), where R is the angle dependent reflection coefficient. Depending on the offset x_h this expression includes the primary (pre- or post-critical reflection) and the headwave. In applying the $f - k$ migration algorithm to the data, we make use of a slightly modified migration operator which is defined in terms of the time derivative of the space-time domain data rather than the data itself, see e.g. (Stolt and Benson, 1986). In the frequency domain this amounts to multiplying by an $i\omega$ factor and hence use the modified data

$$P'(x_h, 0; \omega) = \frac{\omega}{2\pi} \int_{-\infty}^{\infty} dk_h \frac{R(k_h)}{k_z} e^{ik_h x_h} e^{-ik_z z_a}. \tag{5.2}$$

Fourier transforming over the space coordinate we obtain

$$P'(k_h, 0; \omega) = \frac{\omega}{k_z} R(k_h) e^{-ik_z z_a} \delta(k_g - k_s). \tag{5.3}$$

We next apply a phase-shift on both the source and receiver depth coordinates and obtain

$$P'(k_h, z; \omega) = \frac{\omega}{k_z} R(k_h) e^{ik_z(z-z_a)} \delta(k_g - k_s). \tag{5.4}$$

Notice that, consistent with the previous analysis, the phase of the events contains information only about vertical propagation (and hence vertical intercept time τ). Applying the imaging condition by integrating over frequency we find

$$I_1(k_h, z) = R(k_h)\delta(k_g - k_s) \int d\omega \frac{\omega}{k_z} e^{ik_z(z-z_a)}. \tag{5.5}$$

It is obvious at this point that the integral over ω will produce a delta like event at the correct depth z_a. However we can change the variable of integration from ω to k_z hence switching from plain phase-shift migration to $f-k$ migration. The relationship between ω and k_z is

$$\omega = \frac{k_z c}{2} \sqrt{1 + \frac{k_h^2}{k_z^2}} \tag{5.6}$$

and so we also have

$$\frac{\omega}{k_z} d\omega = \frac{c^2}{4} dk_z. \tag{5.7}$$

With this change of variable, and after integrating over k_z, the last integral becomes

$$I_1(k_h, z) = R(k_h)\delta(k_g - k_s)\frac{c^2}{4}\delta(z - z_a). \tag{5.8}$$

This last formula shows that the wavenumber-frequency domain migration procedure with the vertical intercept time $\tau = 0$ imaging condition has placed the angle dependent reflection coefficient at the correct depth for all pre-critical, post-critical and critical events. An additional inverse Fourier transform may be performed to obtain the image in (x, z) space.

6 Analytic example: space-frequency domain migration

For the second example we use the same model described above (see Figure 3). As before we start with the data in the space-frequency domain

$$D(x_h, \omega) = \frac{1}{2\pi} \int_{-\infty}^{\infty} dk_h \frac{R(k_h)}{ik_z} e^{ik_h x_h} e^{-ik_z z_a}. \tag{6.1}$$

The integral above can be approximated using a stationary phase formula to obtain (Aki and Richards, 2002)

$$D(x_h, \omega) = \frac{R(x_h)}{d_0} e^{-i\omega t_R} + A(x_h, \omega) e^{-i\omega t_H}. \tag{6.2}$$

In this equation the first term describes the seismic reflection and the second the headwave which exists for post-critical offsets only (see Figure 4). In the first term, the reflection coefficient R is a function of offset x_h, d_0 represents the total distance from the source to the reflector and to the receiver along a ray-like path and $t_R = d_0/c_0$ represents the total travel-time. In the second term A is an amplitude factor which has the approximate value

$$A(x_h, \omega) = \frac{i}{\omega} \frac{c_0^2}{\left(1 - c_0^2/c_1^2\right)} \frac{1}{r^{1/2} L^{3/2}}, \tag{6.3}$$

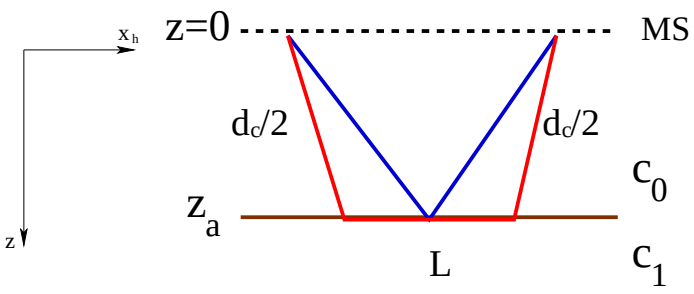

Figure 4: Large offset data consisting of a reflection and a headwave arrival.

with r being the distance between the source and receiver, L being the length of the propagation path of the headwave along the interface, and

$$t_H = d_c/c_0 + L/c_1, \tag{6.4}$$

is the total travel-time for the headwave arrival, with d_c being the total distance from the source to the interface and back to the receiver along the critical ray path (see Figure 4). Notice that in the expression (6.2), consistent with the previous analysis, the phase of each event contains information about the total travel-time of that arrival; this is a direct consequence of expressing the data in the space-frequency domain.

We next apply equation (4.7) to the data described by equation (6.2) and find

$$I_2(x_h, z) = \int dx_h d\omega D(x_h; \omega) \int dk_h e^{i(k_h x_h + k_z z)}. \tag{6.5}$$

Notice that k_z and k_h are no longer independent variables and, in fact, we can consider k_z to be a function of k_h described by the dispersion relations. The inner most integral is approximated using the stationary phase formula

$$\int dk_h e^{if(k_h)} \approx \sqrt{\frac{2\pi i}{f''(k_h^0)}} e^{if(k_h^0)} \tag{6.6}$$

where k_h^0 is the stationary point for $f(k_h)$ found by solving $f'(k_h) = 0$. For our discussion the function f is

$$f(k_h) = x_h k_h + z\sqrt{(\omega/c_0)^2 - k_h^2}. \tag{6.7}$$

Solving the equation $f'(k_h^0) = 0$ we find the stationary point k_h^0 to be

$$k_h^0 = \frac{\omega x_h}{c_0 d} \tag{6.8}$$

where $d = \sqrt{x_h^2 + z^2}$. The values of the function f and of its second derivative f'' at this stationary point are $f(k_h^0) = \frac{\omega}{c_0} d$ and $f''(k_h^0) = -\frac{c_0 d^3}{\omega z^2}$ respectively. Putting all these in formula (6.5) we find the inner most integral to be

$$\int dk_h e^{i(k_h x_h + k_z z)} \approx \frac{z}{d} \sqrt{\frac{2\pi\omega}{i c_0 d}} e^{i\frac{\omega}{c_0} d} \tag{6.9}$$

and so the image I_2 becomes

$$I_2(x_h, z) = \int dx_h d\omega D(x_h; \omega) \frac{z}{d} \sqrt{\frac{2\pi\omega}{ic_0 d}} e^{i\frac{\omega}{c_0}d}. \tag{6.10}$$

With the data given by equation (6.2) the migration procedure yields

$$I_2(x_h, z) = \int dx_h \frac{R(x_h)}{d_0} \frac{z}{d} \sqrt{\frac{2\pi}{ic_0 d}} \int d\omega \sqrt{\omega} e^{i\frac{\omega}{c_0}(d-d_0)} + \int dx_h \frac{z}{d} \sqrt{\frac{2\pi}{ic_0 d}} \int d\omega \sqrt{\omega} A(x_h, \omega) e^{i\omega\left(\frac{d}{c_0} - t_H\right)}. \tag{6.11}$$

The main conclusions inferred from the equation above are that, first, the integration over the frequency ω amounts to a total travel-time imaging condition $t = 0$ and, second, the imaging step places the reflection at the correct and the headwave at the incorrect spatial location. Imaging with $t = 0$ is a direct consequence of the domain of the imaged data, in this case space-frequency, and, even for simple cases, creates false images.

7 Conclusions

In this paper we discuss the application of the imaging principle in depth migration algorithms and its dependence on the domain in which it is applied. We show that an integration over the frequency amounts to a total travel-time $t = 0$ condition when the data is in the space-frequency domain and to a vertical intercept time $\tau = 0$ condition when the data is in the wavenumber-frequency domain. We describe two of the most common depth migration methods representative of the two imaging domains and show that even though their formulation is similar (compare equations (4.6) and (4.7)) involving, besides approximations, only a different integration order, the results can be very different. The two analytic examples we discuss emphasize one important distinction in their ability to handle refracted events (headwaves). This research provides new insights into the mathematical formulation and physical interpretation of depth migration algorithms. Understanding the differences and capabilities of the imaging principles is the key to developing more accurate and complete imaging methods. The results described in this paper impact not only the migration schemes but also others which use the imaging principle implicitly, e.g. inverse scattering methods and in particular the internal multiple attenuation algorithm.

Acknowledgment

The author is grateful to the three anonymous reviewers whose comments helped improve the clarity of this paper. This work was partially supported by NSF-CMG award DMS-0327778 and DOE Basic Sciences award DE-FG02-05ER15697. The author thanks Sam Kaplan for his suggestions in improving this manuscript. M-OSRP support is gratefully acknowledged.

References

Aki, K. and Richards, P. G. 2002. *Quantitative Seismology*, Second Edition, University Science Books.

Bleistein, N. and Hendelsman, R. A. 1975. *Asymptotic Expansions of Integrals*, Holt, Rinehart and Winston.

Claerbout, J. 1981. *Fundamentals of geophysical data processing*, Blackwell Scientific Publications, Inc., New York.

Gazdag, J. 1978. Wave equation migration with the phase-shift method, *Geophysics* **43**(7): 1342–1351.

Nita, B. G. and Weglein, A. B. 2004. Imaging with $\tau = 0$ versus $t = 0$: implications for the inverse scattering internal multiple attenuation algorithm, *74th Annual International Meeting, SEG, Expanded Abstracts* pp. 1289–1292.

Nita, B. G. and Weglein, A. B. 2005. Inverse scattering internal multiple attenuations algorithm in complex multi-d media, *Technical report*, Mission Oriented Seismic Research Project, University of Houston.

Schneider, W. A. 1978. Integral formulation for migration in two and three dimensions, *Geophysics* **43**(1): 49–76.

Stolt, R. H. 1978. Migration by fourier transform, *Geophysics* **43**(1): 23–48.

Stolt, R. H. and Benson, A. K. 1986. *Seismic Migration: Theory and Practice*, Vol. 5 of *Seismic Exploration*, Geophysical Press.

Weglein, A. B., Araújo, F. V., Carvalho, P. M., Stolt, R. H., Matson, K. H., Coats, R. T., Corrigan, D., Foster, D. J., Shaw, S. A. and Zhang, H. 2003. Inverse scattering series and seismic exploration, *Inverse Problems* (19): R27–R83.

Yilmaz, O. 2001. *Seismic Data Analysis: Processing, inversion and Interpretation of Seismic Data*, Society of Exploration Geophysicists.